Proceedings Ninth Workshop Geothermal Reservoir Engineering
Stanford University, Stanford, California, December 1983
SGP-TR-74

RESOURCE EVALUATION AND DEVELOPMENT PLANS FOR A 120 MW GEOTHERMAL POWER PLANT ON MILOS ISLAND, GREECE

M.J. Economides[1], C.A. Ehlig-Economides[1],
G. Speliotis[2], F. Vrouzi[2]

[1]University of Alaska, Fairbanks
[2]Public Power Corporation (Greece),

ABSTRACT

Five deep wells have been drilled on the Island of Milos, Greece, identifying a high-temperature, high-enthalpy geothermal reservoir. The thermodynamic properties of the fluid, and the estimated porosity and presumed thickness of the formation suggest a fluid and heat storage capacity that could support a 60 MWe power plant for 85 years or a 120 MWe for half that time.

The existing five wells can deliver 180 t/h of steam at 10 bar abs pressure, capable of generating a maximum electric power output of slightly less than 20 MWe.

This paper describes the geology, the drilling and the well testing results pertaining to the five wells, and discusses the reservoir potential for a 60 MWe geothermal power plant.

INTRODUCTION

Milos Island, a member of the Cyclades Group in the Aegean Sea, is part of the active Aegean Volcanic Arc of which the islands of Santorini and Nisyros are also members. The Island of Milos and Nisyros have been been the sites of major drilling activity. Figure 1 based on the work by McKenzie[1] shows the location of Milos Island within the volcanic arc in the Aegean Sea.

Two exploratory wells, MA-1 and MZ-1, drilled in 1975-76 proved productive. The former was drilled in the Adamas area, while the latter was drilled in the Zephyria area. Three other wells drilled during 1980-82 (M-1, M-2 and M-3) all proved productive. Figure 2 positions the wells on the map of the island.

GEOLOGY

The Island of Milos may be represented by the generalized model shown on Figure 3 offered by Vrouzi[2]. The schematic represents a W-E cross-section of the island at the latitude of the Zephyria plane. The model shows an infiltration zone in the west (associated with several lava domes), a partial deep discharge towards the east, the development of a series of convective circuits within the reservoir (metamorphic complex), some upward leakages through the main fault systems, a cover made up of widespread hydrothermal alterations of a polygenic formation, and some local intrusions connected with the few domes outcropping in the south-eastern sector of the island. The latter intrusions, however, represent a local hydrogeological disturbance to the deep system.

Because of the reasonably flat surface terrain and the proximity to population centers, the Eastern part of the Island, and especially the Zephyria-Agrilies and the Adamas regions were sited for the contemplated geothermal development.

DRILLING AND SUBSURFACE LITHOLOGY

Table 1 presents a summary of the well diameters and depths for the three newer wells (M-1, M-2, and M-3).
The sequence of terrains crossed by each well is summarized below.

M-1: A shallow interval of alluvia (0-20 m) is made of stratified flood deposits. From 20-60 m there is the chaotic formation made of melange comprised of schists, micaschists, quartz, limestones and extremely altered materials. Beneath this terrain there is a thick metamorphic layer (60 m to T.D.) consisting of schist primarily of the green schist facies. Epidote is a prominent mineral in this complex.

M-2: The alluvia terrain is again a shallow terrain (0-15 m) composed of stratified flood desposits. A thin layer (15-25 m) of grey tuff and other new volcanics is present. From 25-145 m, there is the chaotic formation consisting of a melange of various lithotypes. Metamorphic fragments (quartz, mica-schists, chloro-schists) are

TABLE 1

DRILLING STATISTICS FOR WELLS M-1, M-2, and M-3

Depth	M-1 1180 m	M-2 1381	M-3 1017 m
Well Diameter			
24"	0-99.5 m	0-169 m	0-186 m
17 1/2"	99.5-399 m	169-600 m	186-637
12 1/4"	399-903 m	600-1381 m	637-1017 m
8 1/2"	903-1180 m		

followed by volcanic fragments, some sedimentary blocks and hydrothermal material. Below 149 m (to T.D.) a thick metamorphic formation similar to the one under M-1 is found.

M-3: No alluvia deposits were found in the case of M-3. Instead, a chaotic melange consisting of metamorphic and volcanic fragments is evident (0-20 m).

A volcanic formation (20-125 m) is characterized by intense hydrothermal alteration rendering much of the original structure of the rock unrecognizable.

This layer is underlain by a sedimentary formation (125-173 m) formed by the Neogenic marine ingression. The formation contains carbonaceous quartz arenites, sandstones, arenaceous carbonate rocks, limestones and dolomites and some shales.

Finally, the thick metamorphic layer observed in M-1 and M-2 is found below 173 m (to T.D.).

The terrain sequences found in the three wells is summarized in schematic form in Figure 4. A geologic history of the structures may then be reconstructed.

A pull-apart fault probably caused the block of rock beneath well M-3 to subside, followed by the marine ingression which led to the deposition of the Neogenic formation (125-173 m). Generally, the sediments are well sorted. Sometime later in the geologic history, the magma from a molten rock body under the metamorphic rock complex intruded upward pushing the whole block upward, depositing it above the neogenic formation by uplifting the overlying melange deposits. Another possibility is that magma formed a volcanic cone around the vent above the neogenic sediments. Then melange and alluvial formations were deposited later above the cone.

The location of the M-3 on the top of the hill forming the uplifted horst that borders the Zephyria plain suggests the presence of two faults (see cross-section) around M-3. This hypothesis is further strengthened by the presence of neogenic sediments in M-3 and their absence in M-1 and M-2.

Considering the mineralogy and lithology of the rocks pierced by the wells, it can be suggested that the metamorphic trend is from M-2 to M-3 to M-1.

Presence of calcite mineral above 900 m and its absence at lower depths can be directly related to the pattern of underground water movement.

FLOW AND TRANSIENT PRESSURE WELL-TESTING

The three new wells have been flowtested and Table 2 contains the pertinent flowrate and enthalpy data.

A large number of injection tests have been done on all three wells. Cold seawater was injected and the ensuing buildup of pressure was allowed to fall off. Nine such tests were done for well M-1. The injection time for each was approximately 30 minutes. Nine similar tests were done for M-2 and three more were done for M-3.

The tests were performed at various well intervals for the evaluation of the reservoir transmissivity. Log-log graphs of these tests were utilized as diagnostic tools. Figure 5 is a log-log graph of three injection fall-off tests from M-1, while Fig. 6 is a similar graph of three injection fall-off tests from M-3.

In general, most of the data demonstrate the presence of fractures, as identified by the half-slope behavior on the log-log graph evident at early time. The data trend then flattens out, a frequent indicator of double porosity systems. A "rule of thumb" known as the "double Δp rule" identifies the

TABLE 2

WELL FLOW DATA

	M-1	M-2	M-3
Total Production Rate at 12 kg/cm^2 (175 psi) wellhead pressure	119 t/h	47 t/h	126 t/h
Enthalpy	1450 kJ/kg	2200 kJ/kg	1600 kJ/kg
Quality at 10 kg/cm^2 (150 psi)	0.35	0.71	0.42
Steam Flow Rate	41.7 t/h	33.4 t/h	52.9 t/h
Condensing Power Plant Maximum Electricity Capacity (20,000 PPH/MWe)	4.6 MWe	3.7 MWe	5.8 MWe
Production Interval	900-T.D.	940-T.D.	900-T.D.
Total Dissolved Solids	120,000 PPM	140,000 PPM	130,000 PPM
Bottom-Hole Temperature	323°C	282°C	300°C+
Bottom-Hole Pressure	~ 120 kg/cm^2	~ 120 kg/cm^2	~ 120 kg/cm^2

commencement of the straight line behavior in a semi-logarithmic graph of the data. According to the rule, data following two times the Δp from the deviation from the half slope will fall on a semi-log straight line. Unfortunately, most of the tests were not run for a sufficiently long time for any sustained or even certain appearance of the semi-log straight line as is evident from Figs. 5 and 6. Further, the short duration of the tests limits the value of the data for interpretation of the double porosity behavior. (These tests, run by the contractor, were not designed by the authors of this report.)

The calculated storage capacity of well M-1 is 43 m^3 (8 1/2" by 1180 m). A half hour injection at 100 m^3/h (as it was done for most tests) would barely unload the original wellbore contents into the formation.

Semi-log graphs of the data are presented in Fig. 7. Injection tests #4 and #9 were selected for analysis since they were done over roughly the same completion interval. The extrapolation of the time function $(t+\Delta t)/\Delta t$ to unity (infinite fall-off time, Δt) would result in the initial reservoir pressure). Hence, since the tests were done for the same depth, the extrapolation of these straight lines must converge at approximately the same value of pressure. The slopes for the two straight lines were thus obtained and were calculated as 9 kgr/cm^2/cycle (for test #4) and 3.6 kgr/cm^2/cycle (for test #9).

The pertinent equation for calculating the permeability is:

$$k = \frac{526\, q\mu}{mh} \qquad (1)$$

where k in md, q in m^3/hr, μ in cp and h in m.

The permeability values obtained from these two tests were 11.5 md and 14 md, respectively.

The wellbore drainage factor or skin effect may be calculated using the equation:

$$S = 1.151\left(\frac{p_{1hr}-p_i}{m} - \log \frac{k}{\phi\mu c_t r_w^2} + 3.11\right) \qquad (2)$$

where k in md, μ in cp, c_t in (kgr/cm^2)$^{-1}$ and r_w in m.

Equations 1 and 2 were developed for the above units from the well equations, widely used in petroleum reservoir engineering.

Using Eq. 2, the skin effect for both tests was calculated as S = -7. The negative value for the skin further supports the notion that the well has penetrated a natural fracture.

Injection test #2, done at a shallower interval was also analyzed providing a permeability value of 3.7 md and a skin factor of -6.

The injection tests performed during the drilling operation provided a number of useful results about the formation and the wells. The diagnostic log-log plots gave evidence of the presence of natural fractures, a widespread feature of

geothermal reservoirs elsewhere. The flattening out of the data trends gave indication of two porosity systems also evident in other geothermal formations. Analysis of three of these tests provided estimates for the formation permeability and the open hole wellbore condition. The negative value of the skin effect provided additional evidence of the penetration of natural fractures by the wells.

Short-time injection tests, utilizing alien to the formation fluids (seawater) at much lower temperature would create other phenomena (such as thermal fracturing) that would mask or alter certain formation characteristics. At the present time, drawdown/buildup and interference well tests are contemplated in order to evaluate formation characteristics as well as the principal axes of permeability. The latter are extremely important in any future re-injection schemes which must be planned in conjunction with the development of the power plant.

RESERVE ESTIMATION

Assuming a maximum of 25 km^2 areal extent with a 1000 m thick reservoir (much of it will be accessible through vertical fractures touching the well, not through drilling) a bulk volume of 2.5×10^{10} m^3 may be calculated. Using a porosity value of 5%, the pore volume may then be calculated as 1.25×10^9 m^3. The liquid specific volume at reservoir conditions (p=120 kg/cm^2) is 1.53×10^{-3} m^3/kg. Hence, the mass present is $1.25 \times 10^9 / 1.53 \times 10^{-3}$ or 8.18×10^{11} kg. Since 20,000 lb/hr or 9100 kg/hr have been traditionally used per 1 MWe, the total flow need for a 60 MWe, assuming 50% quality is 1.09×10^5 kg/hr. Hence, the expected longevity of the resrvoir is calculated as 85 years.

DEVELOPMENT PLANS

At the time of writing this paper, the Public Power Corporation is in the first phase of the development of the geothermal reservoirs of Milos, and is in the process of contracting the design and installation of a small 1.5-2 MWe condensing power plant by mid 1985. This pilot facility will provide a means for testing prototype separators, pipelines, turbines, condensers and re-injection schemes for problems associated with scaling and corrosion. In addition, extended fluid production and re-injection will provide more definitive data on the reservoir and on the sustained deliverability and injectivity characteristics of the wells.

The second phase will include the drilling of five new geothermal wells, testing and measurements, the study of a plausible geothermal model and the determination of the total power capacity (expected to be about 60 MWe) resulting in the design, procurement and installation of a 60 MWe power plant by late 1989. The installation of the first network of submarine cables for the transmission of the generated power will also take place during this phase.

The third phase will include the drilling of approximately 20 new geothermal wells, appropriate testing and measurements aiming towards the procurement and installation of a second 60 MWe power plant by late 1992. This phase will include the installation of a second network of submarine cables for the transmission of the additional 60 MWe.

Since the power output is expected to greatly outpace the demand for Milos or that of the islands in its immediate proximity, the installation of the submarine cables for power transmission to the Greek mainland is considered of utmost importance and is contemplated at the present time by the PPC.

REFERENCES

1. McKenzie, D.P.,: "Active Tectonics of the Mediterranean Region: R. Astron. Soc., Geophys. J., v. 30, no. 2. p. 105-185, 1972.

2. Vrouzi, F.: Research and Development of Geothermal Resources in Greece: Present Status and Future Prospects, Public Power Corporation Report, Athens, 1983.

ACKNOWLEDGEMENTS

The authors wish to thank Messrs. Shaukat A. Khan and Timothy Collett for their input in the geological analysis contained herein.

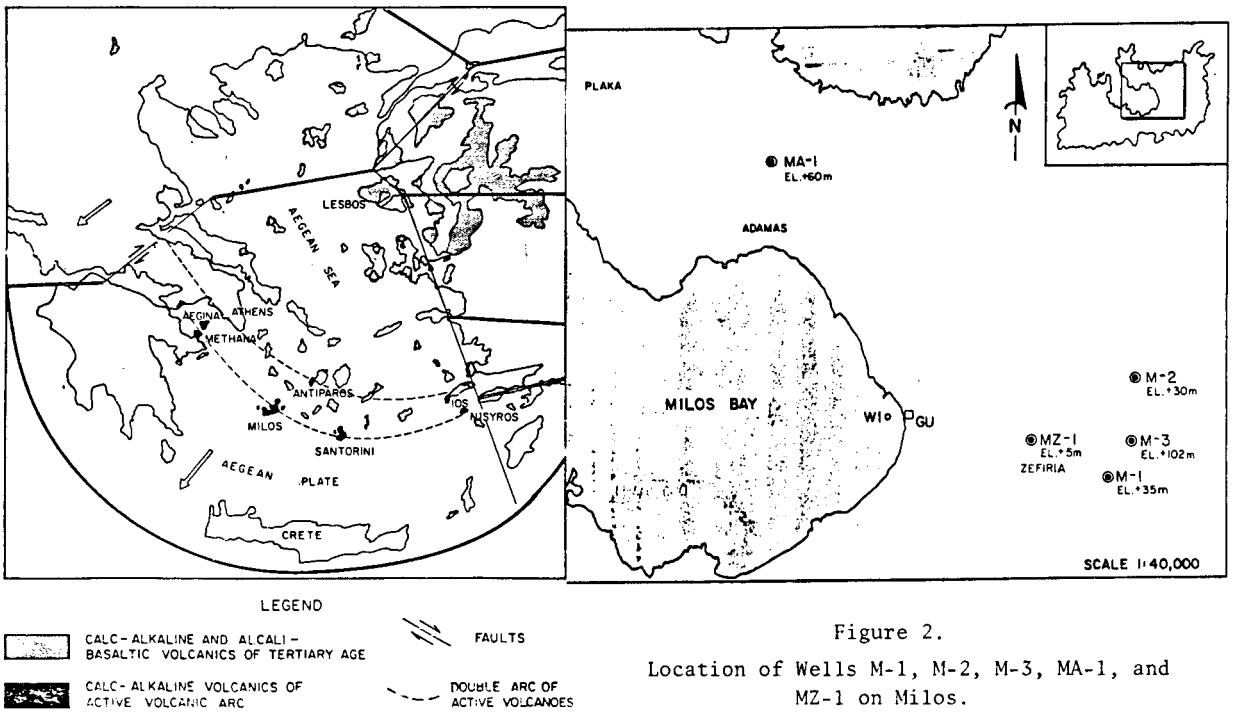

Figure 1.
Distribution of Volcanic Rocks of Tertiary and Quaternary Age in the Aegean Region.

Figure 2.
Location of Wells M-1, M-2, M-3, MA-1, and MZ-1 on Milos.

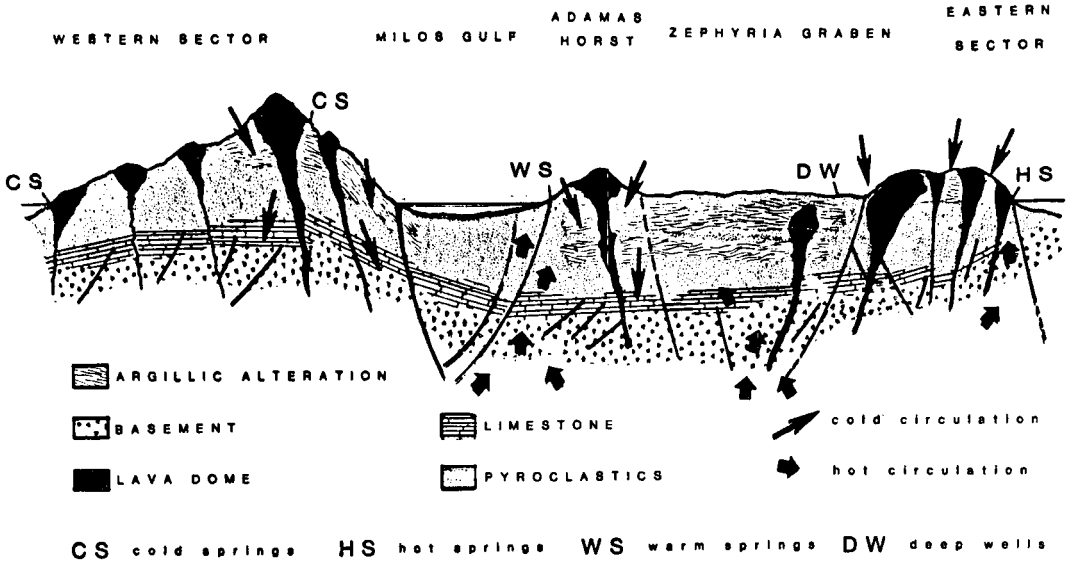

Figure 3.

Sketch of geothermal model of the Island of Milos (From Ref. 2).

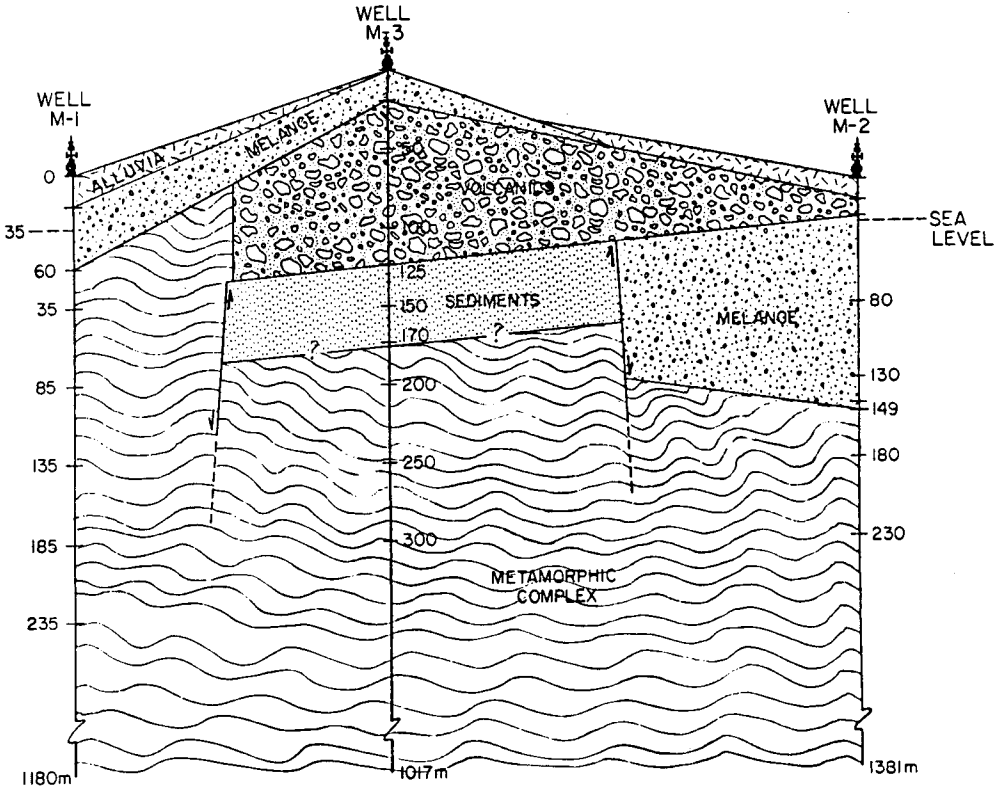

Figure 4

Terrain Sequences penetrated by wells M-1, M-2 and M-3, N-S Cross section.

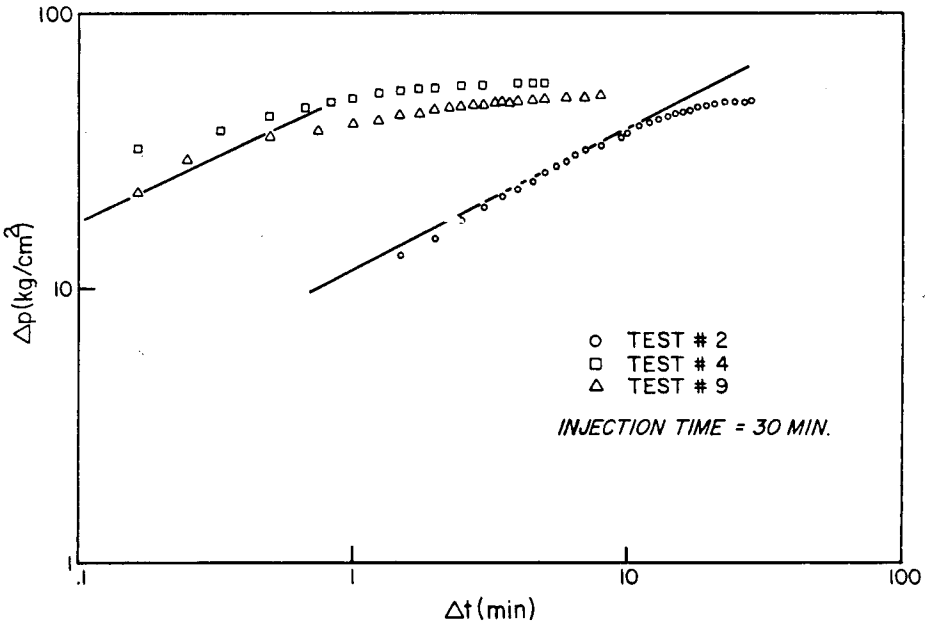

Figure 5
Injection Fall-off Pressure Transients Tests for M-1

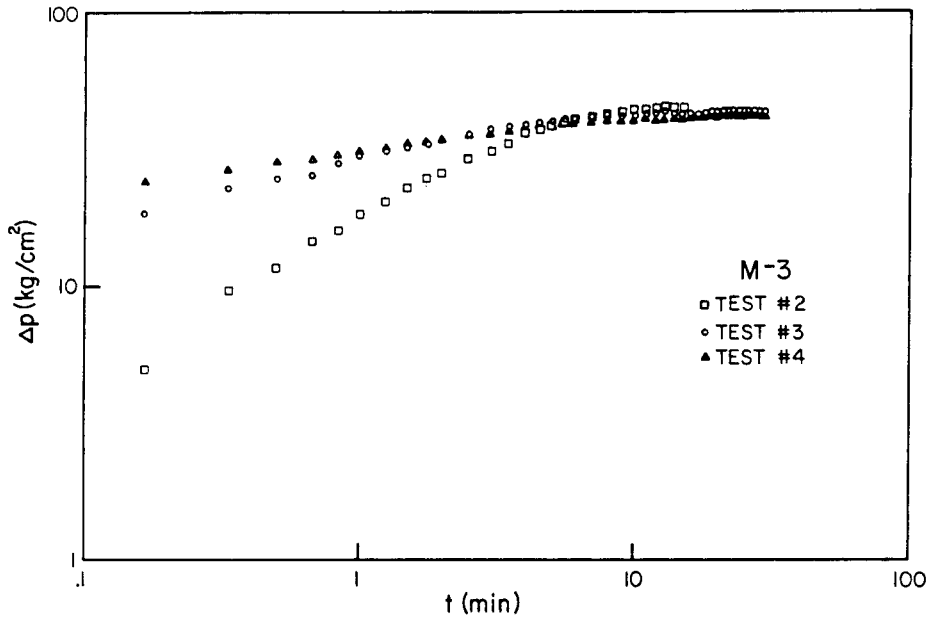

Figure 6
Injection Fall-off Pressure Transients Tests for M-3

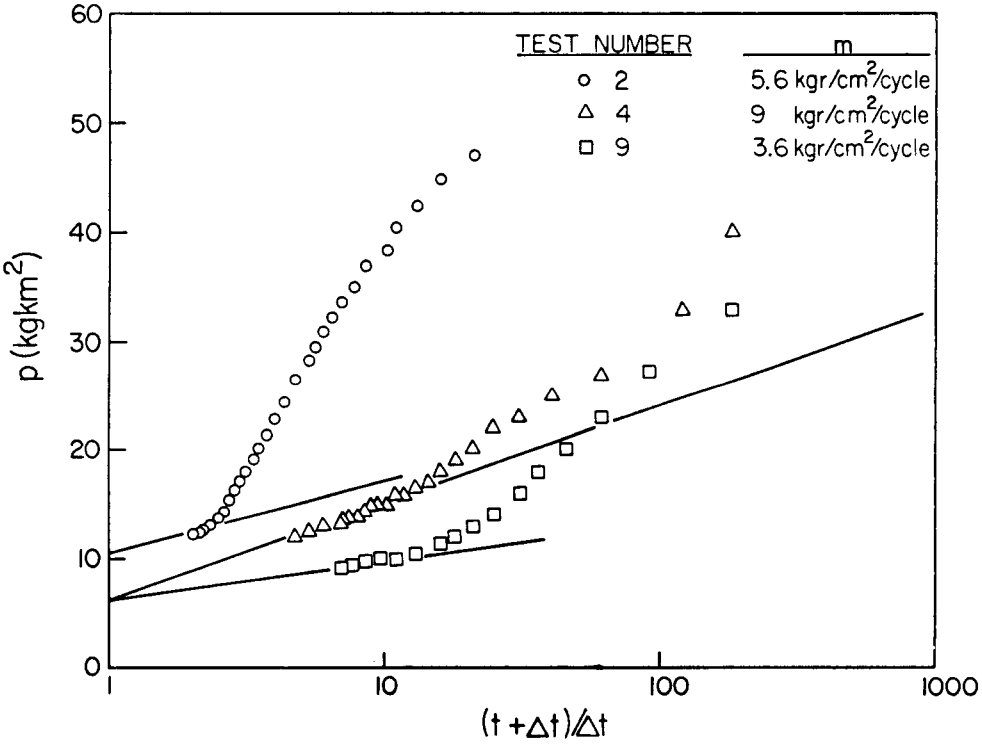

Figure 7
Semi-logarithmic Analysis of Pressure Transients Data for Well M-1.